

# Quantitative Evaluation of the Regional Dynamic Function of Hepatocytes after Living Donor Liver Transplantation Using $^{99m}\text{Tc}$ -GSA: A Preliminary Report

Yasuharu OHNO,<sup>1,2</sup> Haruo ISHIDA,<sup>1</sup> Akira HAYASHI,<sup>1</sup> Shoichiro KAMAGATA,<sup>1</sup> Seiichi HIROBE,<sup>1</sup> Yasushi FUCHIMOTO,<sup>1</sup> Katsumi ISHII<sup>1</sup>

<sup>1</sup>Department of Surgery, Tokyo Metropolitan Kiyose Children's Hospital, Tokyo, Japan

<sup>2</sup>Division of Pediatric Surgery, Nagasaki University Graduate School of Biomedical Sciences, Nagasaki, Japan

In this study, we attempted to evaluate the dynamic function of graft livers after a living donor liver transplantation (LDLT) using technetium-99m-galactosyl-human serum albumin ( $^{99m}\text{Tc}$ -GSA) scintigraphy. We performed  $^{99m}\text{Tc}$ -GSA scintigraphy 24 times in a total of 15 pediatric patients following LDLT. The age at examination (mean  $\pm$  standard deviation) was  $7.3 \pm 5.54$  years. The median interval between the examination and LDLT was 42 months. We converted the time activity curve for the graft to a horizontal mirror image curve and calculated the mean transit time (MTT) and depicted the functional image. The whole graft MTT showed a significant correlation with the receptor index ( $r = -0.528$ ,  $p = 0.014$ ), total bilirubin ( $r = 0.470$ ,  $p = 0.032$ ) and cholinesterase ( $r = -0.641$ ,  $p < 0.014$ ), and a marginally significant correlation with the clearance index ( $r = 0.424$ ,  $p = 0.056$ ). The functional image was quite useful for making a visual evaluation of the regional dynamic distribution of  $^{99m}\text{Tc}$ -GSA in the graft. We thus consider this modality a valuable adjunct for evaluating the regional deterioration of the dynamic function of the liver following liver transplantation.

ACTA MEDICA NAGASAKIENSIA 49: 137–141, 2004

**Keywords:** Liver transplantation; Asialoglycoprotein receptor scintigraphy; Dynamic function of the liver

## Introduction

Technetium-99m-diethylenetriamine-pentaacetic acid-galactosyl-human serum albumin ( $^{99m}\text{Tc}$ -GSA) is a receptor binding agent specific for the asialoglycoprotein receptor that resides exclusively on the plasma membrane of hepatocytes. It provides valuable information on the receptor population density and thus directly reflects the total mass of the functioning hepatocytes.<sup>1,3</sup> However, the conventional indices in  $^{99m}\text{Tc}$ -GSA scintigraphy, including both the clearance and receptor indices,<sup>4</sup> are obtained based on analyses of two fixed points. As a result, the conventional indices can represent the total mass of functioning hepatocytes but may not be able to accurately estimate the regional dynamic function of the liver.

We recently evaluated the regional dynamic function of hepatocytes by introducing the novel parameters in  $^{99m}\text{Tc}$ -GSA scintigraphy for pediatric liver diseases and reported that the mean transit time (MTT) and functional image enabled us to elucidate the regional dynamic function of hepatocytes both quantitatively and visually.<sup>5</sup> In this study, using both MTT and functional imaging, we evaluated the dynamic

function of the graft liver after living donor liver transplantation (LDLT) in pediatric patients. We also assessed the possibility of this modality being used to estimate postoperative complications after liver transplantation (LT).

## Patients and Methods

### Patients

We performed 24 consecutive  $^{99m}\text{Tc}$ -GSA scintigraphies on 15 pediatric patients after LDLT from October 1992 to December 2002 in Tokyo Metropolitan Kiyose Children's Hospital. The patients were 4 boys and 11 girls. The primary diseases were biliary atresia in 12 patients, Wilson's disease in 1, Byler's disease in 1 and glycogen storage disease in 1. The age at examination varied from 1 to 22 years with the mean (standard deviation) of 7.3 (5.54) years. No patients underwent re-transplantation. The interval between the examination and LDLT varied from 4 to 92 months with the median of 42 months. Twenty-four  $^{99m}\text{Tc}$ -GSA scintigraphies were available

**Address correspondence:** Yasuharu Ohno, M.D., Ph.D., Division of Pediatric Surgery, Nagasaki University Graduate School of Medical Sciences, 1-7-1 Sakamoto, Nagasaki 852-8501 JAPAN

TEL: +81-(0)95-849-7316, FAX: +81-(0)95-849-7319, E-mail: y-ohno@net.nagasaki-u.ac.jp

Received May 25, 2004; Accepted December 16, 2004

for analysis in this study. The results of biochemical examinations, which were simultaneously performed along with scintigraphy, were also available for analysis.

#### <sup>99m</sup>Tc-GSA scintigraphy

The 185 MBq of <sup>99m</sup>Tc plus 3 mg of GSA was injected intravenously and dynamic images were recorded with the patient in a supine position under a gamma-camera with a large field of view and a low-energy multipurpose collimator with parallel holes centered on the liver and the precordium. The dose was halved for children under 10 years old. Computer acquisition of the gamma-camera data was started just before the bolus injection of the <sup>99m</sup>Tc-GSA and was stopped 40 minutes later. Digital images (128 × 128 pixels) were obtained at the rate of 30 seconds per frame. The time activity curve (TAC) for the heart and liver were generated from the respective regions of interest (ROI). Except for the long acquisition time, these methods were exactly the same as the conventional methods.

#### Calculation of the conventional indices

The index of blood clearance was calculated by dividing the radioactivity of the heart ROI at 15 minutes after the injection by that of the heart ROI at 3 minutes after the injection. The receptor index was calculated by dividing the radioactivity of the liver ROI by that of the liver-plus-heart ROIs at 15 minutes after the injection.<sup>4</sup>

#### Mean transit time and functional image

The detailed calculations of the unique parameters, the MTT and functional image, in <sup>99m</sup>Tc-GSA scintigraphy have all been reported in our previous paper.<sup>5</sup> In each pixel of the liver ROI, we converted the TAC to a horizontal mirror image curve, which was displayed as a decay curve. Based on the height over area method,<sup>6</sup> the ratio of the peak value of the count to the sum of the counts obtained during decay was automatically computed. Based on the MTT in each pixel, we were thus able to obtain the MTT values in arbitrary ROIs and depict the functional image of the liver. In the functional image, the color scale was made proportionate to the magnitude of 1/MTT in each pixel.

#### Statistical analysis

The data were summarized in the form of mean ± standard deviation. Association between the whole graft MTT and receptor index and biochemical parameters was evaluated by regression analysis. The JSTAT (for Windows, version 6.5) was used for the calculations.

## Results

The results of the acquired data were as follows: whole graft MTT, indicating the mean value of the MTTs in graft ROI — 253 ±

75.5 sec (normal range, <330); receptor index — 0.94 ± 0.054 (normal range, ≥ 0.92); clearance index — 0.51 ± 0.122 (normal range, ≤ 0.57); aspartate aminotransferase — 50 ± 25.4 IU/L (normal range, 8-40); alanine aminotransferase — 47 ± 33.0 IU/L (normal range, 5-35); total bilirubin — 0.58 ± 0.244 mg/dL (normal range, <1.0); and cholinesterase — 291 ± 60.5 U/L (normal range, 120-460).

The whole graft MTT was compared with the conventional <sup>99m</sup>Tc-GSA indices and biochemical data. A significant correlation was observed between the whole graft MTT (y) and receptor index (x) ( $y = -1100.2x + 1304.10$ , Pearson's correlation coefficient ( $r$ ) = -0.528,  $p = 0.014$ ), total bilirubin (x) ( $y = 132.1x + 182.27$ ,  $r = 0.470$ ,  $p = 0.032$ ) and cholinesterase (x) ( $y = -0.66x + 456.83$ ,  $r = -0.541$ ,  $p = 0.014$ ) (Figure 1). The whole graft MTT showed a marginally significant correlation with the clearance index (x) ( $y = 243.6x + 138.23$ ,  $r = 0.424$ ,  $p = 0.056$ )

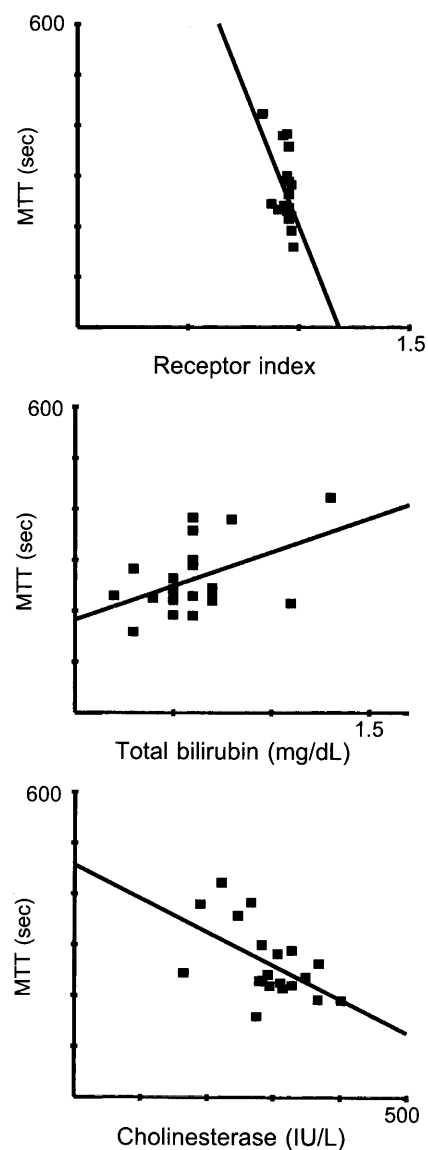


**Figure 1.** Scatter plots of the whole graft MTT (mean transit time) and the receptor index (upper panel), total bilirubin (middle panel), and cholinesterase (lower panel).

as well, but it showed no significant correlation with either aspartate aminotransferase (x) ( $y=0.32x+245.22$ ,  $r=0.121$ ,  $p=0.601$ ) or the alanine aminotransferase (x) ( $y=0.32x+246.02$ ,  $r=0.159$ ,  $p=0.490$ ).

Based on the MTT in each pixel, we could depict the functional image of the graft liver, which enabled us to visually appreciate the abnormalities in the regional dynamic function in each pixel. Figure 2 and Figure 3 show the serial follow-up  $^{99m}\text{Tc}$ -GSA images of a 13-year-old girl, who underwent ABO incompatible LDLT for Wilson's disease, taken 10 months and 6 years after the transplantation, respectively.

Ten months after the transplantation, her laboratory data became slightly exacerbated: aspartate aminotransferase was 71 IU/L and alanine aminotransferase was 101 IU/L. Her hepatic functional reserve also seemed to be slightly exacerbated: the clearance index was 0.63; the receptor index was 0.93; and the MTT was 379.2 seconds. The conventional  $^{99m}\text{Tc}$ -GSA image of Figure 2 (A) shows that the accumulation of isotopes is concentric; however, a decreased area

in the central lesion was also observed. Because conventional imaging is highly influenced by the thickness of the liver parenchyma, the hepatic functional reserve cannot be visually expressed. On the other hand, Figure 2 (B) shows a functional image in which a dynamic function of the hepatocytes is homogeneously maintained in the graft. Figure 2 (C), computed tomography, shows a cystic lesion in the graft.<sup>7</sup>

Six years after the transplantation, her laboratory examinations showed no changes: aspartate aminotransferase was 72 IU/L and alanine aminotransferase was 53 IU/L. However, her hepatic functional reserve showed deterioration: the clearance index was 0.77; the receptor index was 0.82; and the MTT was 422.0 seconds. The conventional  $^{99m}\text{Tc}$ -GSA image of Figure 3 (A) shows an expansion of the decreased area in hilar lesion. On the other hand, Figure 3 (B) shows a functional image in which the dynamic function of the hepatocytes was not inconsistently but homogeneously exacerbated in the graft. Figure 3 (C) shows a huge cystic lesion in the hilum.

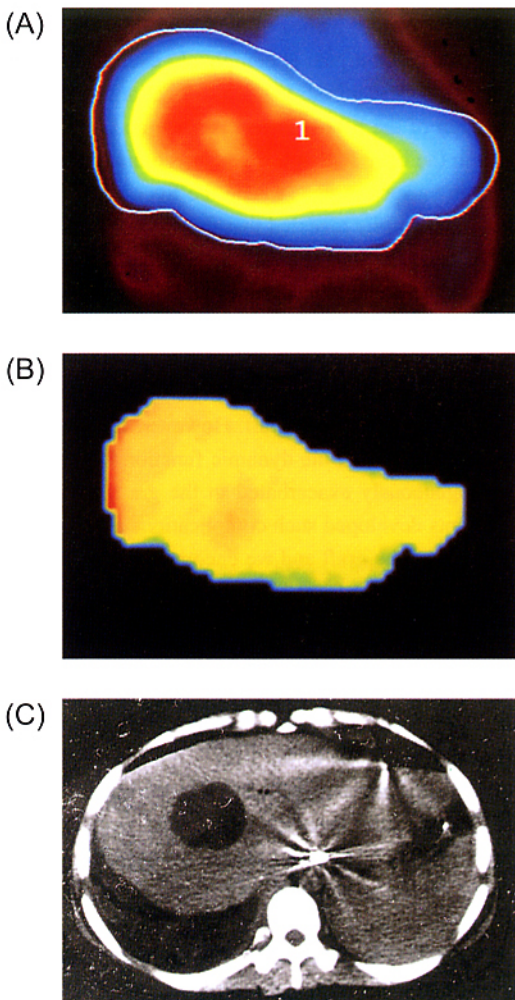


**Figure 2.** The serial  $^{99m}\text{Tc}$ -GSA images of a 13-year-old girl, who underwent LDLT for Wilson's disease, taken 10 months after the transplantation. (A) A conventional  $^{99m}\text{Tc}$ -GSA image. (B) A functional image. (C) A computed tomography image.

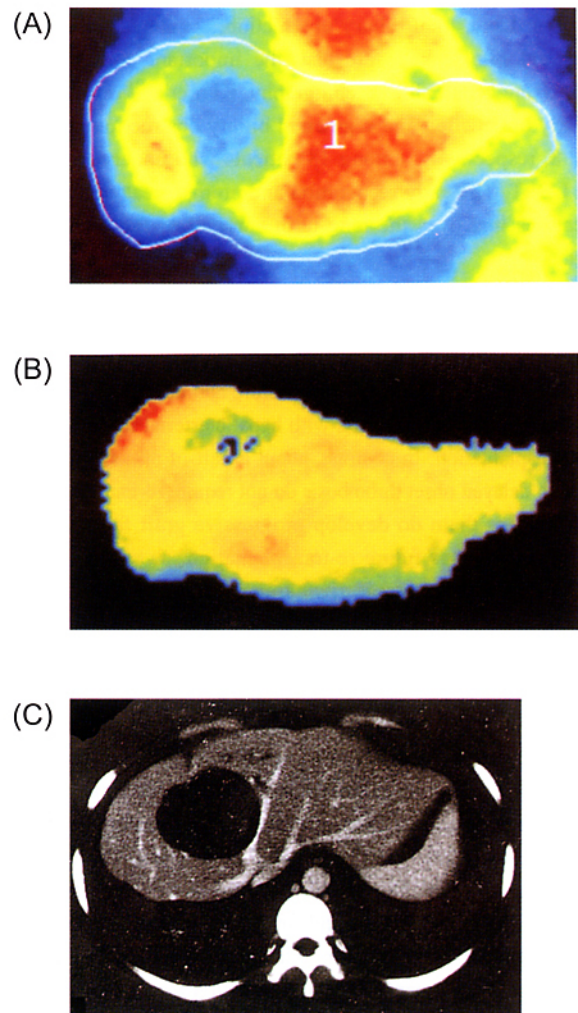


**Figure 3.** The serial  $^{99m}\text{Tc}$ -GSA image taken 6 years after transplantation for the same patients described in Figure 2. (A) A conventional  $^{99m}\text{Tc}$ -GSA image. (B) A functional image. (C) A computed tomography image.

## Discussion

Various postoperative complications following LT have been reported up to now.<sup>8</sup> Such complicated conditions require an exact evaluation of the hepatic functional reserve of the graft and may also be a source of significant morbidity, often necessitating re-transplantation. On the other hand, the surgical complications that cause a dysfunction of the limited area of the graft liver are also important because a prompt surgical correction may be necessary. However, these complications are difficult to diagnose accurately and treat appropriately. Therefore, in this study, we assessed the possibility of using MTT and functional imaging as an alternative modality for evaluating postoperative complications after LT.

Venous or biliary complications following LT may lead to acute and chronic liver injury.<sup>9,10</sup> In LDLT patients using a right liver graft, the middle hepatic vein is usually separated from the right liver graft, which may thus result in venous congestion in a major part of the right paramedian sector.<sup>11,12</sup> The veno-occlusive area is demonstrated to be so large and hence venous reconstruction should be considered. On the other hand, total biliary obstruction, segmental biliary obstruction and bile leakage are also the important complications after LT. Using hepatobiliary scintigraphy, Kim et al.<sup>13</sup> reported that total biliary obstruction and segmental biliary obstruction occurred in 6 and 8, respectively, among 38 patients who underwent adult-to-adult LDLT. The early recognition and prompt treatment of such complications improves the long-term survival of the patient and the graft.

Hepatic artery thrombosis is also one of the serious complications after LT. It causes a deterioration in the viability of the graft and also causes serious ischemic changes in biliary system thus resulting in such problems as cholangitis, biliary stricture and abscess.<sup>14,15</sup> The majority of the symptomatic patients with hepatic arterial thrombosis require re-transplantation. In contrast, about a half of all asymptomatic patients with delayed onset thrombosis do not require re-transplantation, although 20% of them do develop progressive graft failure which eventually necessitates future re-transplantation.

Auxiliary partial orthotopic liver transplantation (APOLT) has been developed to overcome the small-for-size graft problem in the treatment of fulminant hepatic failure. Regeneration of the native liver occurs in about 70 % of APOLT patients,<sup>16</sup> and complete recovery of the native liver may make such patients no longer need immunosuppressants.<sup>17</sup> As a result, at the postoperative management of APOLT, it is almost inevitable to monitor the serial hepatic functional reserve in the native and graft livers independently.<sup>18</sup>

The conditions following LT or APOLT as described above necessitate the diagnostic modalities which allow for an accurate evaluation of the hepatic functional reserve and strict assessment of the regional dynamic function of the liver as an indicator of a prompt surgical intervention. Numerous quantitative liver function tests have been developed but no reliable test of the hepatic functional reserve, which provides accurate prognostic information about graft function following LT, has yet been developed.<sup>19</sup> Several researchers have come up with various ideas to assess the dynamic function of the

liver using pharmaceuticals or <sup>99m</sup>Tc-GSA scintigraphy.<sup>4,18,20-24</sup> We believe these analyses to be valuable; however, not all analyses may be consistent since they are either inappropriate for evaluating the regional function or are generally cumbersome for public use because they require custom-made instruments or complicated calculations. Ideally, regional dynamic functional test should be easy to perform and analyze, and should have simple pharmacokinetic profile and high predictive value with quick results.

Planar <sup>99m</sup>Tc-GSA scintigraphy is an examination of the total number of functioning hepatocytes of the whole liver and thus it is not able to accurately estimate the regional dynamic functional reserve.<sup>18</sup> We therefore developed a new method for MTT and functional imaging using <sup>99m</sup>Tc-GSA scintigraphy both to assess the dynamic function of hepatocytes and to estimate the regional function of the liver.<sup>5</sup> Based on the height over area method, the MTT value in each pixel is calculated using the same method as that employed in a pulmonary ventilation study.<sup>6</sup> The distinctive features in our modality employed in this study are as follows: (1) it is based on the dynamic functional assessment in each pixel, calculated only by the TAC of the liver; (2) the influence of the blood flow and the thickness of the hepatic parenchyma is completely excluded and no attenuation correction is required; (3) using functional imaging, the virtual recognition of the heterogeneity is easy; and (4) we can set arbitrary ROIs in the liver so that it is easy to compare the dynamic function between various regions inside the liver.

In this study, our results revealed that the whole graft MTT correlates with the receptor index, total bilirubin and cholinesterase. We also described a patient who was complicated with cyst formation after LDLT. The functional reserve of the graft had gradually become exacerbated. Conventional <sup>99m</sup>Tc-GSA imaging may cause misunderstandings that the hepatic functional reserve deteriorated locally in the hilar lesions of the graft. However, functional imaging enables us to realize that the dynamic function is not inconsistently but homogeneously exacerbated in the graft. In this study, because no patients developed such complications as a dysfunction of the limited area of the graft and we encountered no APOLT patients, we could not think of a typical functional image with a regional deterioration of the dynamic function after LT. However, by using the same modality, we were able to confirm that a 19-day-old patient with biliary atresia at an extremely early stage of the disease showed a deterioration of the regional dynamic function which was only limited to the right lobe of the liver.<sup>5</sup>

Our previous study<sup>5</sup> evaluating the MTT in the pediatric patients with various types of liver diseases reported a significant correlation between whole liver MTT and clearance index. However, the correlation between the whole graft MTT and the clearance index in the present study was only marginally significant, although no significant difference was observed in the two correlation coefficients. This was probably due to the difference in the number of patients.

The methodology for calculating MTT and the method of administering <sup>99m</sup>Tc-GSA we used in the previous study<sup>5</sup> was questioned by Humphrey R. Ham<sup>25</sup> in his letter to the editor of *The Journal of*

Nuclear Medicine. However, in the previous study, we only applied the principle of the height over area method and did not evaluate the retention function. We also consider that TAC obtained under the same condition, either continuous or bolus administration of  $^{99m}\text{Tc}$ -GSA, should be valuable in the clinical evaluation. We developed a new examination, which we termed MTT. This wording, however, may confuse the readers since the term of MTT has been in common use for a long time in pulmonary ventilation study.

A significant correlation observed between the whole graft MTT and receptor index suggests that MTT may serve as an indicator of hepatic functional reserve. This, however, remains to be resolved since in the present study we did not evaluate the MTT as an indicator of hepatic functional reserve.

In conclusion, we consider the modality described in the present study a valuable adjunct to evaluate the regional deterioration of the dynamic function of the liver following either LT or APOLT. This diagnostic modality can be used virtually at all medical institutions because it only requires slight modification of the analytical program already in public use for pulmonary ventilation studies.

## Acknowledgements

We thank Mr. Brian Quinn for reading the manuscript.

## References

1. Kwon AH, Ha-Kawa SK, Uetsuji S, Kamiyama Y, Tanaka Y. Use of technetium  $^{99m}$  diethylenetriamine-pentaacetic acid-galactosyl-human serum albumin liver scintigraphy in the evaluation of preoperative and postoperative hepatic functional reserve for hepatectomy. *Surgery* 117: 429-434, 1995
2. Kudo M, Todo A, Ikekubo K et al. Functional hepatic imaging with receptor-binding radiopharmaceutical: clinical potential as a measure of functioning hepatocyte mass. *Gastroenterol Jpn* 26: 734-741, 1991
3. Kwon AH, Ha-Kawa SK, Uetsuji S, Inoue T, Matsui Y, Kamiyama Y. Preoperative determination of the surgical procedure for hepatectomy using technetium- $^{99m}$ -galactosyl human serum albumin ( $^{99m}\text{Tc}$ -GSA) liver scintigraphy. *Hepatology* 25: 426-429, 1997
4. Ha-Kawa SK, Tanaka Y, Hasebe S et al. Compartmental analysis of asialoglycoprotein receptor scintigraphy for quantitative measurement of liver function: a multicentre study. *Eur J Nucl Med* 24: 130-137, 1997
5. Ohno Y, Ishida H, Hayashi A, Kamagata S, Hirobe S, Ishii K. The mean transit time and functional image in asialoglycoprotein receptor scintigraphy: a novel modality for evaluating the regional dynamic function of hepatocytes. *J Nucl Med* 43: 1611-1615, 2002
6. Suga K, Nishigauchi K, Kume N et al. Dynamic pulmonary SPECT of xenon-133 gas washout. *J Nucl Med* 37: 807-814, 1996
7. Colina F, Castellano VM, Gonzalez-Pinto I et al. Hilar biliary cysts in hepatic transplantation. Report of three symptomatic cases and occurrence in resected liver grafts. *Transpl Int* 11: 110-116, 1998
8. Yamanaka J, Lynch SV, Ong TH et al. Surgical complications and long-term outcome in pediatric liver transplantation. *Hepatogastroenterology* 47: 1371-1374, 2000
9. Sugimoto H, Kaneko T, Marui Y et al. Reversal of portal flow after acute rejection in living-donor liver transplantation. *J Hepatobiliary Pancreat Surg* 8: 573-576, 2001
10. Fulcher AS, Turner MA, Ham JM. Late biliary complications in right lobe living donor transplantation recipients: imaging findings and therapeutic interventions. *J Comput Assist Tomogr* 26: 422-427, 2002
11. Inomata Y, Uemoto S, Asonuma K, Egawa H. Right lobe graft in living donor liver transplantation. *Transplantation* 69: 258-264, 2000
12. Sano K, Makuuchi M, Miki K et al. Evaluation of hepatic venous congestion: proposed indication criteria for hepatic vein reconstruction. *Ann Surg* 236: 241-247, 2002
13. Kim S, Moon H, Lee G et al. The usefulness of hepatobiliary scintigraphy in the diagnosis of complications after adult-to-adult living donor liver transplantation. *Eur J Nucl Med* 29: 473-479, 2002
14. Valente JF, Alonso MH, Weber FL, Hanto DW. Late hepatic artery thrombosis in liver allograft recipients is associated with intrahepatic biliary necrosis. *Transplantation* 61: 61-65, 1996
15. Bhattacharjya S, Gunson BK, Mirza DF et al. Delayed hepatic artery thrombosis in adult orthotopic liver transplantation-a 12-year experience. *Transplantation* 71: 1592-1596, 2001
16. Jaeck D, Boudjema K, Audet M et al. Auxiliary partial orthotopic liver transplantation (APOLT) in the treatment of acute liver failure. *J Gastroenterol* 37: 88-91, 2002
17. Fujita M, Furukawa H, Hattori M, Todo S, Ishida Y, Nagashima K. Sequential observation of liver cell regeneration after massive hepatic necrosis in auxiliary partial orthotopic liver transplantation. *Mod Pathol* 13: 152-157, 2000
18. Sakahara H, Kiuchi T, Nishizawa S et al. Asialoglycoprotein receptor scintigraphy in evaluation of auxiliary partial orthotopic liver transplantation. *J Nucl Med* 40: 1463-1467, 1999
19. Jalan R, Hayes PC. Review article: quantitative tests of liver function. *Aliment Pharmacol Ther* 9: 263-270, 1995
20. Oellerich M, Armstrong VW. The MEGX test: a tool for the real-time assessment of hepatic function. *Ther Drug Monit* 23: 81-92, 2001
21. Nanashima A, Yamaguchi H, Shibasaki S et al. Measurement of serum hyaluronic acid level during the perioperative period of liver resection for evaluation of functional liver reserve. *J Gastroenterol Hepatol* 16: 1158-1163, 2001
22. Kira T, Tomiguchi S, Takahashi M. Quantitative evaluation of the regional hepatic reserve by  $^{99m}\text{Tc}$ -GSA dynamic SPECT before and after chemolipiodolization in patients with hepatocellular carcinoma. *Ann Nucl Med* 12: 369-373, 1998
23. Matsuzaki S, Onda M, Tajiri T, Kim DY. Hepatic lobar differences in progression of chronic liver disease: correlation of asialoglycoprotein scintigraphy and hepatic functional reserve. *Hepatology* 25: 828-832, 1997
24. Ichihara T, Maeda H, Yamakado K et al. Quantitative analysis of scatter- and attenuation-compensated dynamic single-photon emission tomography for functional hepatic imaging with a receptor-binding radiopharmaceutical. *Eur J Nucl Med* 24: 59-67, 1997
25. Ham HR. Mean transit time and functional image in asialoglycoprotein receptor scintigraphy. *J Nucl Med* 44: 1707, 2003